Clinical Plasma Medicine 7–8 (2017) 16–23

Contents lists available at ScienceDirect

Clinical Plasma Medicine

journal homepage: www.elsevier.com/locate/cpme

Original research article

Human health risk evaluation of a microwave-driven atmospheric plasma jet as medical device

A. Lehmann*, F. Pietag, Th. Arnold

Leibniz Institute of Surface Modification, Permoserstrasse 15, 04308 Leipzig, Germany

ARTICLE INFO

Keywords:
Atmospheric plasma
Plasma medicine

ABSTRACT

Purpose: The aim of this study was the characterisation of a microwave-driven atmospheric plasma jet (APJ) dedicated for medical applications. The scientific focus includes harmless sterilization of surfaces and therapeutic treatments in dentistry.

Methodes: The plasma was investigated with respect to potential health risks for human beings, which could occur especially by the gas temperature, heat flow, patient leakage current, UV emission and ozone emission from the plasma jet, according to DIN SPEC 91315:2014-06 (General requirements for plasma sources in medicine) [1].

Results: The results of the experiments indicate a high potential of the plasma jet to be used as a medical device exhibiting low gas temperatures up to 34 °C. The calculated leakage currents are mostly below the 10 µA threshold. The limiting UV exposure duration for the APJ with a calculated maximum effective irradiance of 2.6 µW/cm2 is around 19 min, based on the exposure limits of the international commission on non-ionizing radiation protection guidelines (ICNIRP) [2]. A significant ozone concentration was observed mainly in the axial effluent gas flow. Ozone concentration strongly decreases with increasing distance from the plasma source exit nozzle.

Conclusion: The investigated APJ exhibits physical properties that might not constitute health risks to humans, e.g. during treatment in dentistry. Thus, the APJ shows a high potential for application as a device in dental therapy.

1. Introduction

Beside the wide range of plasma application in many fields extensively described by Woedtke et al. [3], the medical applications of atmospheric plasmas are ever-expanding in the last years. The scientific focus in the medical field includes among others plasma coagulation [4–6], wound healing [7–9], preventive medicine for decontamination, sterilization and disinfection in healthcare [10–13], experimental cancer research [14–19], in HIV research [20] as well as sterilization and therapeutic treatments in dentistry [21]. Contemporary aspects of plasma application in dentistry, like the modification of dental implant surfaces, enhancing of adhesive qualities, decontamination, root canal disinfection and tooth bleaching, were described and reviewed by different authors [22–24]. The successful application of our atmospheric plasma jet (APJ) in dental experiments has been published in several scientific articles focusing on the effective removal of biofilms, killing of adherent oral microbes, and surface activation of teeth [25–29]. The biological effectiveness of APJ on a wide range of important oral microorganisms has been successfully tested (*Lactobacillus casei*, *Streptococcus mutans*, *Candida albicans* and *Escherichia coli*). *Escherichia coli* were included as reference [27]. Surface temperatures occurring during APJ irradiation were measured by means of infrared-camera thermoscopy (Optris PI, Optris, Germany) at the point of contact to the respective sample surfaces. Hence, temperatures below the biological tolerance threshold were assured. However, in order to ensure a commercial launch with CE marking in future, among others an expansive risk evaluation of APJ is necessary as first step [30]. The estimation of risk factors allows the comparison of different plasma sources and clarifies future minimal standards [31]. In the present paper the APJ is characterised with respect to risks for patients according to DIN SPEC 91315:2014-06 (General requirements for plasma sources in medicine) [1], which standardises a set of experiments in order to estimate the health hazard potential of APJs due to their physical and chemical properties namely gas temperature, thermal output and heat flow to treated surface, patient leakage current, UV radiation and ozone emission.

* Corresponding author.
E-mail address: antje.lehmann@iom-leipzig.de (A. Lehmann).

https://doi.org/10.1016/j.cpme.2017.06.001
Received 1 March 2017; Received in revised form 19 May 2017; Accepted 1 June 2017

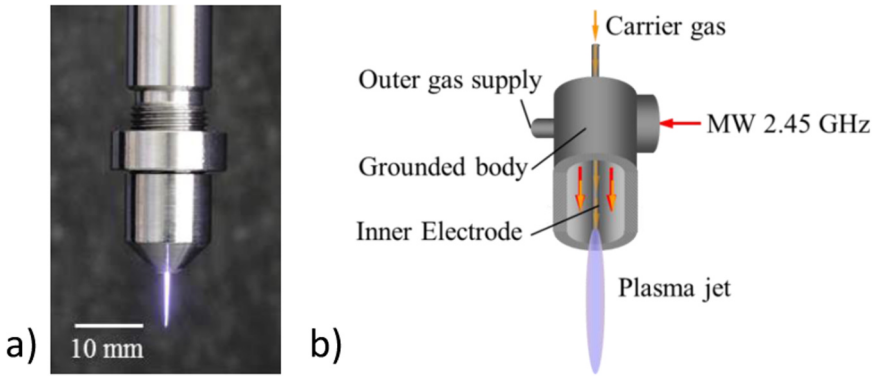

Fig. 1. a) Atmospheric pressure plasma jet – APJ (IOM, Leipzig, Germany); made by NTG GmbH, Gelnhausen, Germany, b) sketch of the APJ source.

2. Material and methods

2.1. Atmospheric plasma jet (APJ)

The plasma system comprising the plasma source and a 2.45 GHz microwave pulse generator used for the investigations has been described earlier by Lehmann et al. [26]. Microwave power was coupled into the plasma source in the form of rectangular pulses by a coaxial cable, where pulse peak power (P_P) was 200 W and the pulse repetition frequency (f_P) was 1.46 kHz. The pulse width (t_P) was adjusted to 5 µs. The used parameters resulted in a mean input power (P_M) of 1.5 W according to Eq. (1):

$$P_M = t_P \cdot P_P \cdot f_P \quad (1)$$

Pulse shape and frequency were monitored using an oscilloscope (TPS2024, Tektronix, Bracknell, U.K.). The carrier gas was helium with gas flow rates of 1.5, 2.0 or 3.0 slm. Nitrogen was used as peripheral shielding gas with flow rates between 0.2 and 0.4 slm. With the given set of electrical and gas parameters a plasma jet was generated exhibiting a visible length of 7–8 mm and a diameter of approx. 1 mm (see Fig. 1a). A sketch of the plasma source under investigation is shown in Fig. 1b. All measured quantities described below were determined along the jet axis for different distances from the nozzle exit (working distance).

2.2. Gas temperature

Plasma gas temperature is a main factor to characterize an atmospheric plasma source especially for medical applications. For this application cold plasmas are used. In literature [32–34] the temperature model of such non-thermal low temperature plasma discharges is described. One of the main characteristic of these plasmas is that the applied electrical energy primarily generates energetic electrons. These energetic electrons produce excited species, ions, as well as additional electrons. In case of cold plasma jets the entire gas stream is less heated than in thermal plasmas, since heavy particles are slightly heated by a few elastic collisions [33] and remain in a low-energetic state [35].

The temperature measurements were carried out by means of a FOTEMP1-4, fiber optic temperature monitoring system (Optocon AG, Germany). The fiber optic thermometer offers complete immunity to microwave radiation [36]. Hence, undisturbed measurement values are ensured. The temperature-sensitive fiber tip was 1 mm in diameter. Hence, the system is suitable for spatially resolved determination of plasma gas temperatures. Data sample rate was chosen to be 1/s. For measurement of the radial temperature distributions two perpendicular cross section line scans of the APJ across the fiber optic were carried out with a scan velocity of 0.1 mm/s.

Axial temperature distribution at the respective positions of the maximum radial temperature was recorded at intervals of 1 mm along the visible jet axis, between distances of 1 mm and 5 mm.

2.3. Heat flow

Measurements of the plasma jet heat flow were accomplished utilizing the fiber optic temperature monitoring system mentioned in the section above, while the fiber tip was connected to a copper body (mass m: 0.35 g; thermal capacity c_w: 385 J/kg K) according to DIN SPEC 91315. The heat flow (P) of the APJ was determined by fitting the slope of the transient temperature curve $\Delta T/\Delta t$ in the near-linear region during the heating-up phase and calculating P according to

$$P = m \cdot c_w \cdot \Delta T/\Delta t. \quad (2)$$

Fig. 2 shows an example of a transient temperature measurement. The experimental setup is shown in Fig. 3a.

2.4. Patient leakage current

The DIN SPEC 91315 [1] refers to IEC DIN EN 60601 [37] in order to evaluate the patient leakage current from the plasma jet. Equipment's provided with not more than one connection to a particular mains supply and used for compensation or alleviation of disease, injury or disability have to be certificated according to IEC DIN EN 60601 [37]. An investigation according to this fundamental norm in Europe [54] is necessary to ensure save operation of the plasma jet as medical-electrical equipment [9]. In Table 1 the regulatory limits of patient leakage current for standard condition (N.C.) and single fault condition (S.F.C.) for devices of type B are given. Type B describes a component (body), which is not designed to transmit current to human body however a power transmission is conceivable [38]. Four types of leakage currents are described (ground leakage current, housing leakage current, patient leakage current, and patient auxiliary current), whereas in this study only the patient leakage current for standard condition was examined.

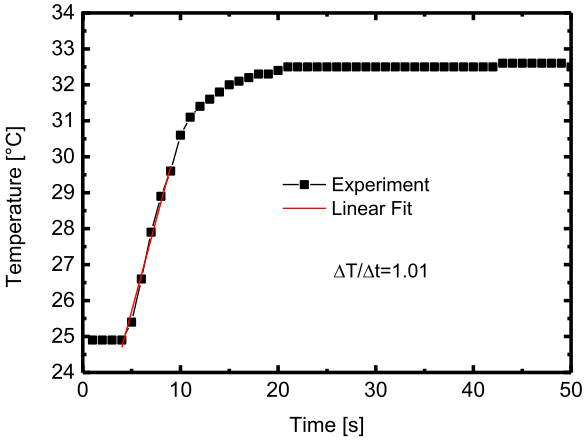

Fig. 2. Example for calculation of the heat flow of the APJ.

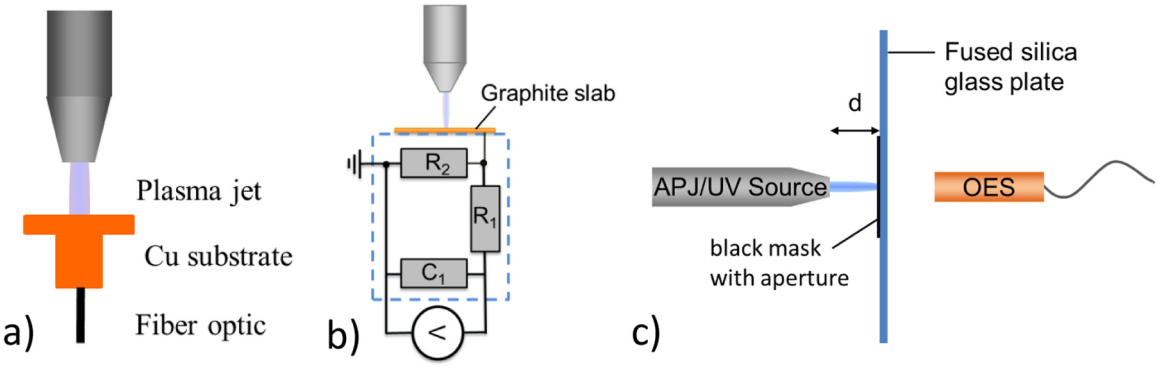

Fig. 3. Experimental setups, a) for calorimetric measurements, b) electrical human body model and c) for UV emission measurements.

Table 1
Regulatory limits of patient leakage current according to IEC DIN EN 60601 for devices of type B.

	Type B	
	Standard condition (N.C.)	Single fault condition (S.F.C.)
AC	10 µA	50 µA
DC	100 µA	500 µA

An overview of effects of current on human beings and livestock is published by DIN VDE V 0140-479-1 [39]. For the human body resistance the simplified human body model described in IEC DIN EN 60601-1 according to Eisner et al. [40] was built (see Fig. 3b). An isolated graphite slab served as an electrically conducting surface which was carried by a metal box containing the electric circuit emulating the body resistance. This circuit consists of resistor R_2 (1 kΩ), followed by an RC-filter formed by resistor R_1 (10 kΩ) and capacitor C_1 (0.015 µF). Such a circuit takes into account the human body and the risk of ventricular fibrillation [40]. The transmitted current was determined by the measurement of voltage V. The resulting patient body leakage currents were calculated from the monitored transient voltage by integration over time, as follows:

$$I_{Pulse} = \frac{1}{t_{int}} \sum_{t=0}^{t_{int}} \frac{|V(t)|}{R_2} \cdot \Delta t \quad (3)$$

$$I_{Leakage} = I_{Pulse} \cdot t_{int} \cdot f_P \quad (4)$$

where I_{Pulse} is the current pulse, t_{int} the integration time, V the voltage, Δt the inverse count rate and f_P the pulse repetition frequency.

2.5. UV emission

Medical application of ultraviolet radiation is found e.g. in dentistry for photocuring of composites by UVA, and in dermatology (all UV bands) [41]. Since atmospheric plasmas are known to emit UV radiation, it is necessary to obtain a quantitative measure of UV light emitted by the gas discharge. The international commission on non-ionizing radiation protection guidelines (ICNIRP) is an independent organization of scientific experts for advising and guiding about health and environmental effects from non-ionizing radiation (NIR) (which means electromagnetic radiation), in order to protect people and the environment from it. The limits in this guideline were based on scientific data [2]. In order to quantify the UV radiation in terms of an irradiance E (W/cm^2) for continuous exposure of eye and skin generated by the plasma, we have regarded the ICNIRP guidelines on limits of exposure to ultraviolet radiation of wavelengths between 180 nm and 400 nm (incoherent optical radiation). Therefore, optical spectroscopic measurements were performed. An optical spectrometer (AOS 4-1, IFU GmbH, Germany) was employed that is capable to detect radiation in a wavelength range of 250–800 nm. The spectral range of 250 nm to 400 nm was investigated, since it includes the following types of UV emission bands: UVC between 100 nm to 280 nm, UVB from 280 nm to 315 nm, and UVA from 315 nm to 400 nm [12], respectively. The range between 100 nm and 250 nm could not be observed because of spectral limitations of the spectrometer. The experimental setup (Fig. 3c) described in DIN SPEC 91315 was adopted for these measurements. The quantitative determination of the effective irradiance and permissible exposure time to skin within an 8 h period is described in detail by the ICNIRP. Measured spectral irradiance E_λ (µW cm^{-2} nm^{-1}) of a broad band UV source is weighted against the relative spectral effectiveness, which is a function of spectral weighting factors $S(\lambda)$ to obtain the effective irradiance E_{eff} (µW/cm^2). Since ultraviolet radiant exposure in the spectral region 180–400 nm incidents upon the unprotected eyes should not exceed 3 J/cm^2, the permissible exposure time in seconds may be computed by dividing the limit mentioned above by E_{eff} [2,42].

In order to calibrate the spectral intensity scale of the spectrometer, reference measurements were carried out using a calibrated spot light UV source (LC8 HAMAMATSU PHOTONICS K.K., Japan). The UV light source associated with the condenser lens E7658-01 and set to 50% of irradiance emits an integrated irradiance of 169 mW/cm^2 at a center wavelength of 365 nm and a distance d of 10 mm in front of the exit lens. Assuming a linear response from the spectrometer detector within the spectral range of 250 nm to 400 nm the integrated intensity of APJ spectra can be normalized to the integrated intensity of the UV lamp.

A fused silica glass plate with thickness of 2 mm was located at a distance d of 10 mm in front of the spectrometer entrance lens for measurements of UV light emerging from the lamp as well as from the APJ. The glass plate was equipped with a black mask exhibiting a circular aperture of 1.5 mm in diameter in order to maintain equal solid angle conditions for the detection of radiation from both UV sources under investigation. A sketch of the experimental configuration for UV emission measurements of the APJ is shown in Fig. 3c.

2.5.1. Ozone emission

Ozone is generated in atmospheric plasma jets by its reactive species that react with the oxygen of the surrounding air. It is on the one hand side an antimicrobial effective gas for air disinfection in food industry [43,44]. Beside reactive oxygen species (ROS) and reactive nitrogen species (RNS), UV radiation, electrical fields and currents, ozone has a direct impact on the cells of microorganisms [45] and effects superficial tissues [46]. The concentration of ozone is strongly depending on the used parameters, like device setup, power of plasma excitation and gas composition [47]. On the other hand, ozone is an important toxic gas with harmful effects to human respiratory. According to EU directives (2002/3/EG) ozone constitutes no health risk at concentrations up to 0.055 ppm (110 µg/m^3), or by Suva up to 0.1 ppm for long-time exposition, usually over a period of eight hours, respectively [31,42].

For the measurements of the ozone concentration generated by the APJ a Thermo Environmental Instruments Model 49C Ozone Analyzer

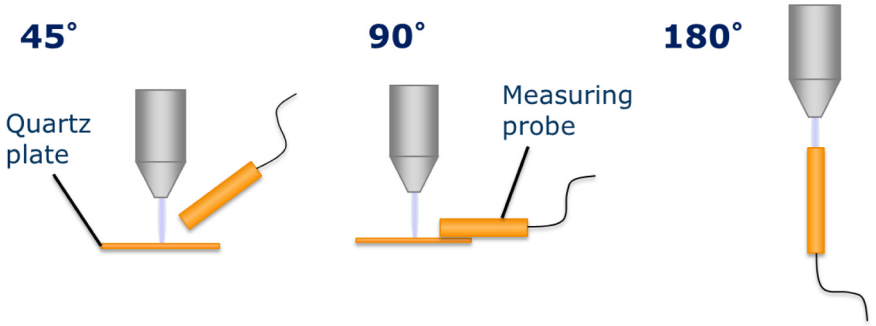

Fig. 4. Experimental setup for detection of ozone concentrations at different measuring angles.

Thermo Scientific, Germany was used. It measures ozone concentrations via UV absorbance at 254 nm with a precision of 1 ppb in a range of 0–0.05 to 200 ppm. The actual ozone concentrations were detected under three different measuring angles at a fixed distance of 10 mm between APJ and the probe as well as in dependence of different distances between the plasma source and the ozone probe on the jet axis at 180°. The experimental setups were arranged according to DIN SPEC 91315 and are shown in Fig. 4.

3. Results

3.1. Temperature measurements

Temperature measurements were carried out at fixed power parameters and varying gas flow parameters. An example of a radial temperature profile is shown in Fig. 5a. From the respective measured radial temperature profiles the maximum temperatures at the working distances were calculated. The results for the axial temperature distribution are shown in Fig. 5b. A cooling effect is supported by the transient discharges using short electric pulses, followed by pulse pauses with not ignited gas stream. As expected, a temperature decrease is observed resulting from an increase of the gas flow. The gas flow is applied through the discharge zone; hence the plasma temperature remains low because of convective cooling [48]. The inner diameter of the micro-wave powered inner capillary pipe is 0.314 mm. For an estimation of the flow condition we have calculated the exit flow Reynolds numbers of the inner gas stream as follows:

$$\mathrm{Re} = \frac{VL}{v} \tag{5}$$

[49], where V is the mean fluid velocity, L the inner diameter of the tube and v is the kinematic viscosity of helium [50] according to the in situ measured jet temperature at a distance of 1 mm for each gas flow rate, respectively. Table 2 shows the data for kinematic viscosity from literature and the calculated Reynolds numbers. In literature, the Reynolds number of approximately 2000 is referred as the "critical" Reynolds number (Re_{cr}) for a transition from laminar to turbulent flow regime [51,52]. The results exhibit the transition from laminar jet conditions at 1.5 slm and 2.0 slm He-flow rates towards to a turbulent regime at a He-flow rate of 3.0 slm.

Table 2
Calculated Reynolds numbers *Re*, according to the He-flow rate and the kinematic viscosity [50].

He-flow rate [slm]	Kinematic viscosity [m^2/s]	Re
1.5	1.4181×10^{-4}	1430
2.0	1.3950×10^{-4}	1937
3.0	1.3360×10^{-4}	3037

All graphs in Fig. 5b show a temperature gradient with the working distance. An ascending temperature profile with the maximum temperature of 59 °C near the tip of the APJ was registered at gas flow rates of 1.5 slm He and 0.2 slm N_2. An increased gas flow of 2.0 or 3.0 slm He and 0.2 or 0.4 slm N_2 led to gas temperatures profiles which decrease towards the visible plasma jet tip. Thereby, the temperature gradient is higher with increasing turbulent gas flow of 3.0 slm He. For the highest gas flow rates temperatures in the range of 34 °C at the tip to 44 °C near the plasma source were obtained. This allows applications in a biocompatible regime. Furthermore, the diagrams show that the visible jet length was influenced by the gas flow. High flow rates resulted in longer visible length (approx. 8 mm). All final measurement points represent the visible length of the plasma jet.

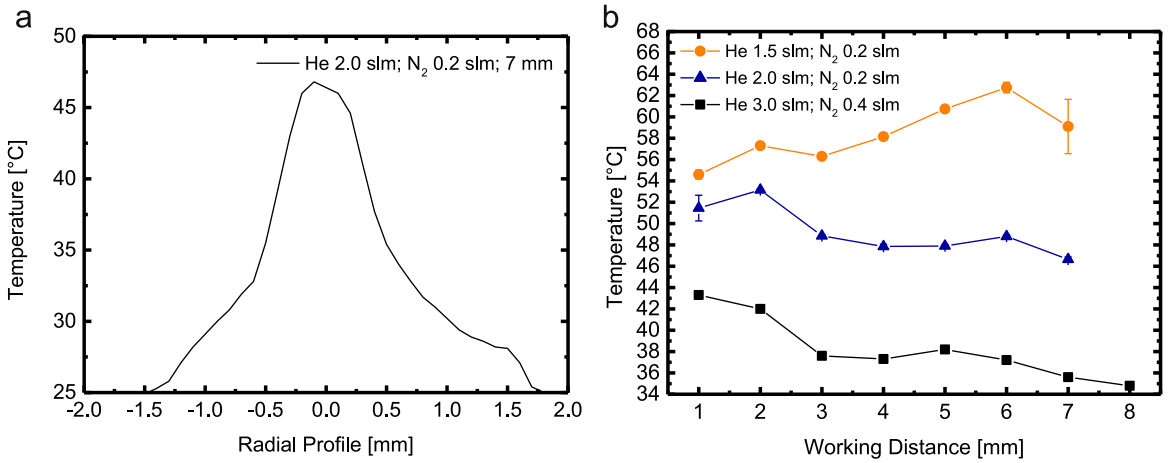

Fig. 5. Temperature measurements by means of fiber optic thermometer, a) radial jet profile and b) maximum temperatures along the APJ axis from nozzle to plasma tip for each gas parameter.

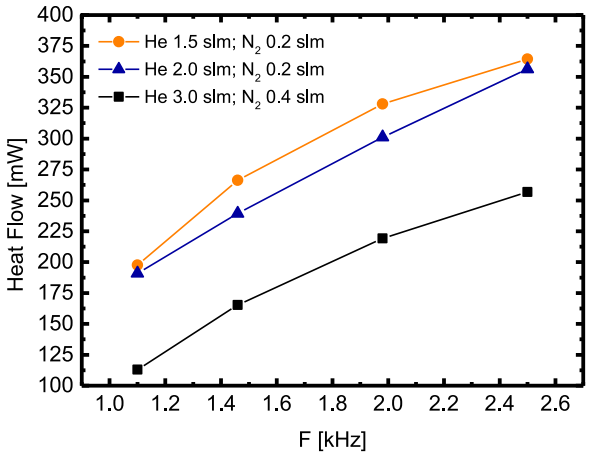

Fig. 6. Calorimetric measurements for evaluation of the heat flow of APJ, taken at 3 mm from the nozzle with variation of frequency.

3.2. Measurement of heat flow

For these measurements the same set of gas flow parameters were adjusted as for the temperature measurements. No significant changes of the heat flow in dependence of the distance between the copper body connected to the fiber optic and the plasma jet source was detected. Therefore the axial distance for measurements presented in Fig. 6 was fixed to 3 mm.

With this gas flow and working distance parameters, the influence of the pulse repetition frequency was tested (Fig. 6).

The heat flow significantly increases at rising pulse repetition frequencies and decreasing gas flows, indicating the large influence of the total gas flow rate for cooling the plasma irradiated surface. Analogously to temperature measurements a decrease of the heat flow was observed by the increase of the gas flow rate from 2.0 slm to 3.0 slm He and 0.2 slm to 0.4 slm N_2, respectively.

With respect to the application temperature, the favored application parameters of 1.46 kHz and a flow rate of He of 3.0 slm and N_2 of 0.4 slm show a thermal output of about 165 mW which is similar to results in literature [31]. In addition to results of temperature measurements, this set of parameters seems to be optimal for effective but harmless application being independent of the distance of the plasma source to the surface.

3.3. Measurement of leakage current

Leakage currents are main factors of concern in the application of electrical devices to the human body. Electrical current has very different effects to human bodies. Beside the controlled medical application electrical current flowing through the body can cause a slight tingling right up to stimulation of muscles and nerves, resistive heating of tissue and electrochemical burns or even electric shock [53,54]. Different influence of ambient conditions, such as the humidity and conditions of skin, the size of contact area and the dwell time play an important role. In literature an average total resistance of skin and internal resistance of 1 kΩ (AC) are described [53,55]. The threshold currents are described by DIN EN 60601 to be 100 µA (DC) and 10 µA (AC) [25,38]. Fig. 7 shows an example of the average of 128 single voltage pulses measured with the human body resistance model depicted in Fig. 3b, where variable positions along the APJ axis and a gas flow rate of 3.0 slm of He and 0.4 slm N_2, respectively, were chosen. The graphs clearly show the influence of the RC-filter. The originally input pulse length of 5 µs (marked by the grey box) turns into a current pulse with a rise time of about 18.6 µs. Further it can be seen, that the voltage appears more negative in distance range from 1 mm to 5 mm and turns to positive again at 6 mm. Atmospheric plasma jets show a

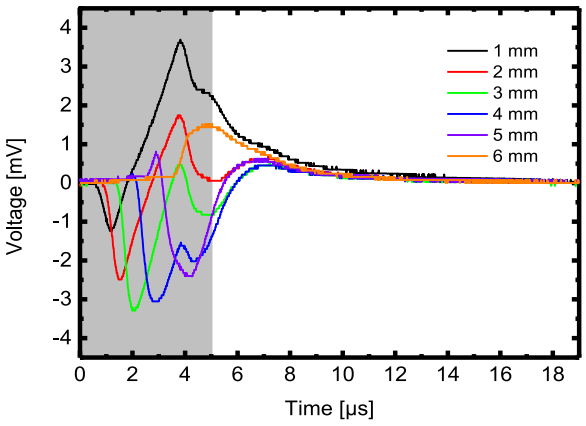

Fig. 7. Average of 128 single voltage pulses measured at human body resistance model from Fig. 3b at different axial distances from the plasma source nozzle.

visible plasma zone (active plasma region), which contains primarily energetic electrons and reactive species, like OH, N_2^* and N_2^+ (see Fig. 9) [56,57]. A closer look to the electron properties and dynamics in atmospheric helium plasma jets is given by Hübner et al. [58] and Boeuf et al. [59]. The working distance of 6 mm is in region of the tip of the visible jet. At this distance a transition from the active plasma region into a more positive plasma afterglow occurs. There the air proportion is much higher [60,61] and relative long-living radicals, like OH, O, O_3, NO and more [56] are present.

Fig. 8 shows the calculated leakage current along the APJ axis as well as for varied gas flows from the data in Fig. 7. All graphs show the same trend. The calculated leakage currents are mostly below the threshold of 10 µA. Obviously, the gas flow has a significant influence to the patient body leakage current. The leakage current increases with increasing gas flows at the jet axis between 2 mm and 6 mm.

3.4. Measurement of UV emission

Optical emission spectra from 250 nm up to 800 nm were measured at different axial positions of the APJ with gas flows of He of 3.0 slm and N_2 of 0.4 slm (Fig. 9). The spectra consist mainly of atomic emission lines and molecular bands which can be attributed to He, the second positive system of N_2, and OH [41,62].

The UV emission was quantified on a basis of these spectra between 250 nm and 400 nm. Within the spectral limitations of the spectrometer no emitted lines were detected between 250 and 290 nm (UVC region). UVB and UVA emission lines between 295.8 nm and 400 nm were detected and can be ascribed to the second positive system of N_2 [62] and

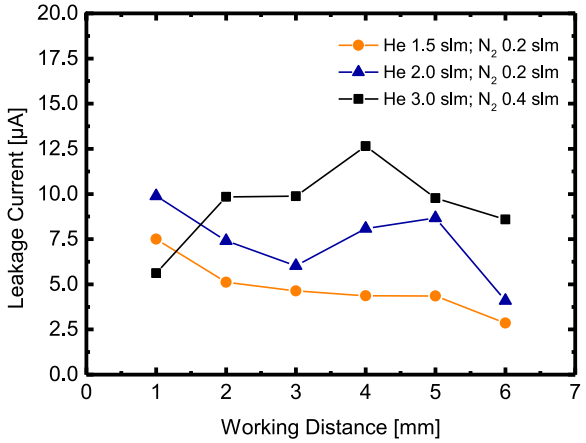

Fig. 8. Leakage current measurements at different working distances along the APJ axis.

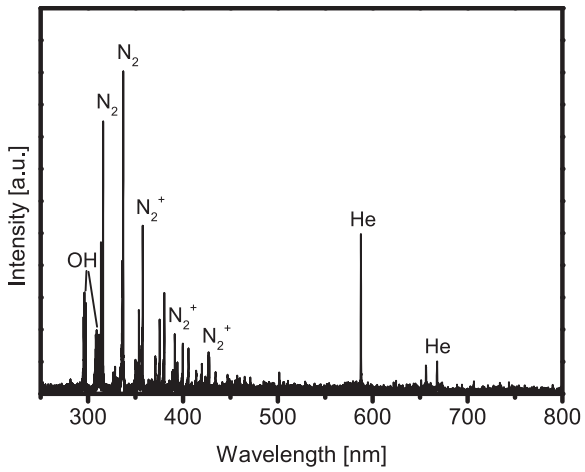

Fig. 9. Optical emission spectrum of APJ between 250 nm and 800 nm.

first order ultra violet OH band [41]. The presence of OH is due to natural water vapor in the open air system.

Fig. 10 shows the calculated irradiance of the APJ between 250 and 400 nm depending on the working distance. The maximum calculated effective irradiance (E_{eff}) at a distance of 1 mm is 2.6 μW/cm^2. Towards the distance of 5 mm, E_{eff} is decreasing to 1.9 μW/cm^2. The limiting UV exposure duration for the APJ with a maximum effective irradiance of 2.6 μW/cm^2 is around 19 min, based on the exposure limits of the international commission on non-ionizing radiation protection guidelines (ICNIRP) [2].

3.4.1. *Measurement of ozone concentration*

Fig. 11 shows the result of the ozone measurements at the APJ for three different measuring angles with respect to the jet axis (45°, 90° and 180°).

Measurements at angles of 45° and 90° show no significant differences with values between 0.7 and 1.7 ppm. However, the ozone concentrations in direction of the APJ axis (180°) show strong increase. At the lowest gas flow the highest concentration of 16 ppm was detected. The change of ozone concentration depending on the axial distance between the plasma source and the gas probe is shown in Fig. 12. It reveals that the ozone concentration is similarly decreasing for all gas flow rates with the distance down to values of around 4 ppm at a distance of 16 mm.

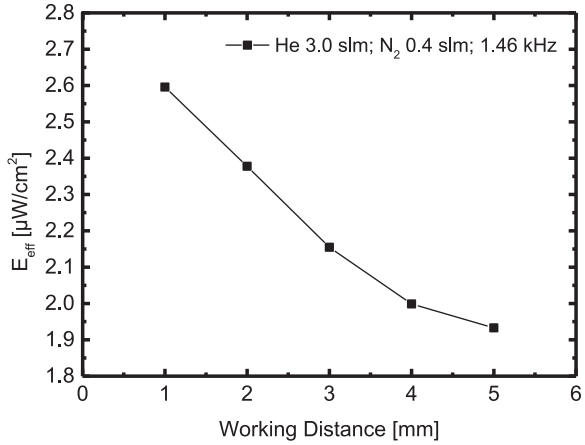

Fig. 10. Irradiance *Eeff* of the APJ in dependence of the working distances (in range of 250–400 nm).

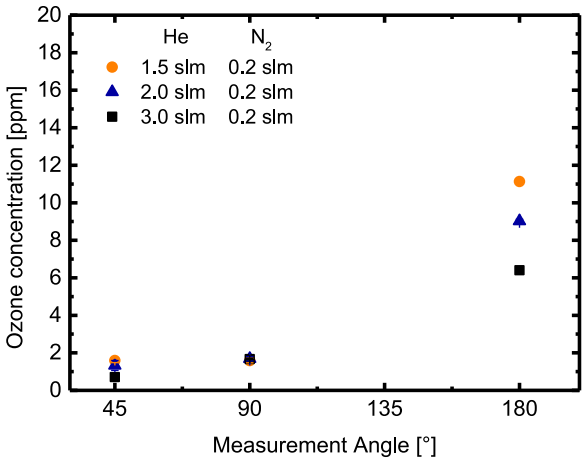

Fig. 11. Ozone concentration measured under different angles at a distance of 10 mm to the plasma source.

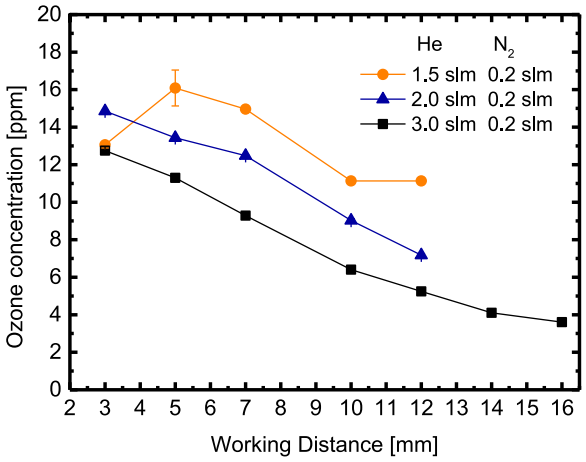

Fig. 12. Ozone concentration at a measuring angle of 180° with varying distances of the probe to plasma source.

4. Discussion

The presented study gives an overview of features of the APJ as a potential medical device. Different investigations were done to evaluate the risk for humans during a treatment by APJ.

The APJ works at patient-friendly temperatures and the thermal output of about 165 mW is similar to results in literature [31]. The low gas temperature is caused by high gas flow rates and low input power. Mentioned above, the temperature gradient is higher with increasing gas flows. Cheng et al. [19] describes the characteristics of the laminar argon plasma jet impinging normally upon a flat substrate located in air surroundings. The plasma parameters (temperature, axial velocity, mass fraction, etc.) are affected by the presence of a substrate, mainly in the near-substrate region. The decay rates of these plasma parameters at a turbulent impinging jet are often appreciably larger than in laminar jets, because more ambient air is entrained into the turbulent jet [19]. In case of the investigated plasma jet we observed a lager gradient of the jet temperature at a gas flow rate of 3.0 slm of He, which is more turbulent than the others.

For the leakage current measurement a simple equivalent circuit of human body resistance has been assumed. The resistance depends on different factors, such as current path, temperature, humidity of skin, size of contact area. Not all of these factors have been considered in the present study. However, especially humidity of skin is a main factor at medical applications. In future an adapted equivalent circuit of human body impedance is necessary for specific applications. Further

Table 3
Comparison of the used APJ with different CE marked cold plasma medical devices,.

	Unit	APJ	kINPen MED®	Plasma Derm®	Micro Plaster β
Plasma generation		Microwave plasma jet	DC plasma jet	Volume DBD	Microwave plasma torch
Plasma gas		He, N_2	Ar	Ambient Air	Ar
Gas flow	[slm]	3, 0.2–0.4	5		2.2
Working distance	[mm]	3	7–10	Millimeter	1
Plasma gas temperature	[°C]	38	35–40		< 40 °C at a distance of 20 mm
Heat fLow	[mW]	165	145–160, at the visible tip of plasma jet		
Effective UV irradiation	[μW/cm^2]	2.6	35 ± 5	0.04	21.1
Leakage current*	[μA]	10	< 50	100	
Ozone concentration	[ppm]	< 1.6 and < 12.5, depending on measurement direction	> 0.2 and (< 0.055 at larger distances)	< 100 μg/m^3	
Reference			[31,63]	[64]	[65,66]

kINPen MED® (INP Greifswald/neoplas tools GmbH, Greifswald, Germany), Plasma Derm® VU-2010 (CINOGY GmbH, Duderstadt, Germany) and Micro Plaster β (Adtec Healthcare©), Hounslow, UK.; Leakage current in * rms (root mean square).

investigations according to IEC DIN EN 60601 (classification of applied parts, type B) are necessary in order to ensure save operation of the plasma jet as medical-electrical equipment.

Optical emission investigations have shown an occurrence of dominant nitrogen bands in the region of UVB and UVA, due to the admixture of nitrogen as shielding gas. However, according to [2] an application of this APJ for about 19 min is possible with the calculated irradiance E_{eff} of 2.6 μW/cm^2. That is sufficient for antimicrobial applications in dentistry, as described by Rupf et al. [22]. Weltmann et al. [31] discussed that the exposure limits and threshold values are dependent on the velocity and the movement of the plasma source over the skin and the condition of the skin. Furthermore, Weltmann et al. [31] and Brandenburg et al. [47] describe a strong variation of UV emission depending on feed gas conditions and capillary outlet especially for atmospheric pressure plasma. For that reason all plasma devices have to be carefully evaluated for the dedicated medical application.

Despite of the nitrogen shielding a significant ozone concentration mainly at a measuring angle of 180° was observed. This has to be taken in to account in the final implementation of a medical device.

A further important point of future investigations is the measurement of microwave leakage of this equipment. With usually used measurement devices (Microwave Survey Meter MM3001B-110AB, Muegge, Germany) we have not detected microwave radiation, yet. Time resolved measurements are proposed to detect the microwave power per pulse.

According to DIN SPEC 91315, these results provide a first estimation of the applicability of the APJ as medical plasma source. In literature, two basic plasma device principles were described, established in research and also used in first practical applications: the volume dielectric barrier discharge (DBD) and the atmospheric pressure plasma jets (APPJ) [3,9,35]. A comparison of the used APJ with different CE marked cold plasma medical devices is shown in Table 3. Beside the different application parameters of atmospheric plasmas, the resulting tested physical criteria can be seen. Different working conditions result for each plasma source with respect to the physical and chemical plasma characteristics, for instance coming from the different discharge and electrode configuration, type of plasma and gas as well as the used excitation frequency [57].

5. Conclusions

In summary, the investigated APJ exhibits physical properties that might not constitute health risks to humans, e.g. during treatment in dentistry. Thus, the APJ shows a high potential for application as a device in dental therapy. It motivates further investigation, e.g. certification by ISO 13485 and the risk assessment according to DIN EN ISO 14971 in order to accomplish the required Medical Device Directive (MDD) for CE marking.

Ethical Statement

Not applicable for this article.

Conflict of interest

The authors have no conflict of interest to declare.

Financial disclosure

On behalf of all authors I certify that we have no financial interest to declare.

Acknowledgements

The authors want to thank Dr. T. Berndt for supply of the ozone measurement system and Dr. U. Decker for supply of the UV spot light. This study was supported by grants from the Zentrales Innovations Programm Mittelstand (ZIM - BMWI), Germany (BMWI; FKZ KF207401KJ3).

References

[1] DIN SPEC 91315, General Requirements For Plasma Sources In Medicine, 2014, pp. 1–16.
[2] ICNIRP GUIDELINES, On Limits of exposure to ultraviolet radiation of wavelengths between 180 nm and 400 nm (Incoherent optical radiation), Health Physics, 87(2), 2004, pp. 171–186.
[3] Th von Woedtke, S. Reuter, K. Masura, K.-D. Weltmann, Plasmas for medicine, Phys. Rep. 530 (2013) 291–320.
[4] K. Miyamoto, S. Ikehara, H. Takei, Y. Akimoto, H. Sakakita, K. Ishikawa, M. Ueda, J. Ikeda, M. Yamagishi, J. Kim, T. Yamaguchi, Red blood cell coagulation induced by low-temperature plasma treatment, Arch. Biochem. Biophys. 605 (2016) 95–101.
[5] J. Raiser, M. Zenker, Argon plasma coagulation for open surgical and endoscopic applications: state of the art, J. Phys. D: Appl. Phys. 39 (2006) 3520–3523.
[6] Argon Plasma Coagulation, A New Paragon In Flexibility and Efficiency, ERBE Elektromedizin GmbH, ERBE USA, Inc. 2225 Northwest Parkway, Marietta, GA, 30067-9317.
[7] Y. Akimoto, S. Ikehara, T. Yamaguchi, J. Kim, H. Kawakami, N. Shimizu, M. Hori, H. Sakakita, Y. Ikehara, Galectin expression in healing wounded skin treated with low-temperature plasma: comparison with treatment by electronical coagulation, Arch. Biochem. Biophys. 605 (2016) 86–94.
[8] Y.-W. Hung, L.-T. Lee, Y.-C. Peng, C.-T. Chang, Y.-K. Wong, K.-C. Tung, Effect of a nonthermal-atmospheric pressure plasma jet on wound healing: an animal study, J. Chin. Med. Assoc. 79 (6) (2016) 320–328.
[9] G. Isbary, W. Stolz, T. Shimizu, R. Monetti, W. Bunk, H.-U. Schmidt, G.E. Morfill, T.G. Klämpfl, B. Steffes, H.M. Thomas, J. Heinlin, S. Karrer, M. Landthaler, J.L. Zimmermann, Cold atmospheric argon plasma treatment may accelerate wound healing in chronic wounds: results of an open retrospective randomized controlled study in vivo, Clin. Plasma Med. 1 (2013) 25–30.

[10] J.L. Hueso, V.J. Rico1, J.E. Frías, J. Cotrino, A.R. González-Elipe, Ar + NO microwave plasmas for Escherichia coli sterilization, J. Phys. D: Appl. Phys. 41 (2008) 092002.
[11] G.E. Morfill, M.G. Kong, J.L. Zimmermann, Focus on plasma medicine, New J. Phys. 11 (2009) 115011.
[12] M. Laroussi, F. Leipold, Evaluation of the roles of reactive species, heat, and UV radiation in the inactivation of bacterial cells by air plasmas at atmospheric pressure, Int. J. Mass Spectrom. 233 (2004) 81–86.
[13] M. Laroussi, X. Lu, Room-temperature atmospheric pressure plasma plume for biomedical application, Appl. Phys. Lett. 87 (113902) (2005) 1–3.
[14] D. Xu, X. Luo, Y. Xu, Q. Cui, Y. Yang, D. Liu, H. Chen, M.G. Kong, The effects of cold atmospheric plasma on cell adhesion, differentiation, migration, apoptosis and drug sensitivity of multiple myeloma, Biochem. Biophys. Res. Commun. 473 (4) (2016) 1125–1132.
[15] J.W. Chang, S.U. Kang, Y.S. Shin, K.I. Kim, S.J. Seo, S.S. Yang, J.-S. Lee, E. Moon, S.J. Baek, K. Lee, C.-H. Kim, Non-thermal atmospheric pressure plasma induces apoptosis in oral cavity squamous cell carcinoma: involvement of DNA-damage-triggering sub-G1arrest via the ATM/p53 pathway, Arch. Biochem. Biophys. 545 (2014) 133–140.
[16] M. Keidar, R. Walk, A. Shashurin, P. Srinivasan, A. Sandler, S. Dasgupta, R. Ravi, R. Guerrero-Preston, B. Trink, Cold plasma selectivity and the possibility of a paradigm shift in cancer therapy, Br. J. Cancer 105 (2011) 1295–1301.
[17] S. Mashayekh, H. Rajayi, M. Akhlaghi, B. Shokri, Z.M. Hassan, Atmospheric-pressure plasma jet characterization and applications onmelanoma cancer treatment (B/16-F10), Phys. Plasmas 22 (2015) 093508.
[18] J. Duan, X. Lu, G. He, The selective effect of plasma activated medium in an in vitro co-culture of liver cancer and normal cells, J. Appl. Phys. 121 (2017) 013302.
[19] H.-R. Metelmann, D.S. Nedrelow, C. Seebauer, M. Schuster, T. von Woedtke, K.-D. Weltmann, S. Kindler, P.H. Metelmann, Head and neck cancer treatment and physical plasma, Clin. Plasma Med. 3 (1) (2015) 17–23.
[20] O. Volotskova, L. Dubrovsky, M. Keidar, M. Bukrinsky, Cold atmospheric plasma inhibits HIV-1 replication in macrophages by targeting both the virus and the cells, PLoS One (2016), https://doi.org/10.1371/journal.pone.0165322.
[21] Y. Zhang, Q. Yu, Y. Wanga, Non-thermal atmospheric plasmas in dental restoration: improved resin adhesive penetration, J. Dent. 42 (2014) 1033–1042.
[22] S. Cha, Y.-S. Park, Plasma in dentistry, Clin. Plasma Med. 2 (2014) 4–10.
[23] R.E.J. Sladek, E. Stoffels, R. Walraven, P.J.A. Tielbeek, R.A. Koolhoven, Plasma treatment of dental cavities: a feasibility study, IEEE Trans. Plasma Sci. 32 (2004) 1540–1543.
[24] C. Schaudinn, D. Jaramillo, M.O. Freire, P.P. Sedghizadeh, A. Nguyen, P. Webster, J.W. Costerton, C. Jiang, Evaluation of a non-thermal plasma needle to eliminate ex vivo biofilms in root canals of extracted human teeth, Int. Endod. J. 46 (10) (2013) 930–937.
[25] A.N. Idlibi, F. Al-Marrawi, M. Hannig, A. Lehmann, A. Rueppell, A. Schindler, H. Jentsch, S. Rupf, Destruction of oral biofilms formed in situ on machined titanium (Ti) surfaces by cold atmospheric plasma, Biofouling 29 (4) (2013) 369–379.
[26] A. Lehmann, A. Rueppell, A. Schindler, I.-M. Zylla, H.J. Seifert, F. Nothdurft, M. Hannig, S. Rupf, Modification of enamel and dentin surfaces by non-thermal atmospheric plasma, Plasma Process Polym. 10 (2013) 262–270.
[27] S. Rupf, A. Lehmann, M. Hannig, B. Schäfer, A. Schubert, U. Feldmann, A. Schindler, Killing of adherent oral microbes by a non-thermal atmospheric plasma jet, J. Med. Microbiol. 59 (2010) 206–212.
[28] S. Rupf, A.N. Idlibi, N. Umanskaya, M. Hannig, F. Nothdurft, A. Lehmann, A. Schindler, L.V. Müller, W. Spitzer, Desinfektion und Entfernung oraler Biofilme von mikrostrukturiertem Titan mit kaltem atmosphärischem Plasma. Deutscher Ärzte-Verlag, zzi, Z Zahnärztl Impl, 27(2), 2012, pp. 14–24.
[29] S. Rupf, A.N. Idlibi, F. Al Marrawi, M. Hannig, A. Schubert, L.V. Mueller, W. Spitzer, H. Holtmann, A. Lehmann, A. Rueppell, A. Schindler, Removing biofilms from microstructured titanium ex vivo: a novel approach using atmospheric plasma technology, PLoS One 6 (10) (2011) e25893.
[30] K.-D. Weltmann, Th. v. Woedtke, Basic requirements for plasma sources in medicine, Eur. Phys. J. Appl. Phys. 55 (1) (2011), https://doi.org/10.1051/epjap/2011100452.
[31] K.-D. Weltmann, E. Kindel, R. Brandenburg, C. Meyer, R. Bussiahn, C. Wilke, T.V. Woedtke, Atmospheric pressure plasma jet for medical therapy: plasma parameters and risk estimation, Contrib. Plasma Phys. 49 (9) (2009) 631–640.
[32] C. Tedero, C. Tixir, P. Tristant, J. Desmaison, P. Leprince, Atmospheric pressure plasmas: a review, Spectrochem. Acta Part B 61 (2006) 2–30.
[33] A. Fridman, A. Chirokov, A. Gutsol, Non-thermal atmospheric pressure discharges, J. Phys. D: Appl. Phys. 38 (2005) R1–R24.
[34] A. Rutscher, Characterization of low-temperature plasmas under non-thermal conditions – a short summery, in: R. Hippler, S. Pfau, K.H. Schoenbach (Eds.), Low Temperature Plasma Physics, Fundamental Aspects and Applications, Wiley-VCH Verlag Berlin GmbH, Berlin, 2001, pp. 15–28.
[35] K.-D. Weltmann, Th von Woedtke, Plasma medicine—current state of research and medical application, Plasma Phys. Control Fusion 59 (014031) (2017).
[36] 〈http://www.optocon.de/en/products/fiber-optic-temperature-signal-conditioners/fotemp1-4-fiber-optic-single-channel-thermometer/〉.
[37] DIN EN 60601-1-12:2015, Medical electrical equipment – Part 1-12: General requirements for basic safety and essential performance – Collateral Standard: Requirements for medical electrical equipment and medical electrical systems intended for use in the emergency medical services environment, 2015.
[38] P. Sonntag, 103 | Wirkung des elektrischen Stromes auf den Menschen und Nutztiere, Verlag Europa-Lehrmittel 2008, Aus der Technikredaktion, 1–11.
[39] DIN IEC/TS 60479-1:2007-05, VDE V 0140-479-1:2007-05, Effects of Current on Human Beings and Livestock – Part 1: General Aspects (IEC/TS 60479-1:2005 + Corrigendum October 2006).
[40] L. Eisner, R.M. Brown, D. Modi, Leakage Current Standards Simplified. MDDI in Regulatory and Compliance, 2004.
[41] I.E. Kieft, E.P. v d Laan, E. Stoffels, Electrical and optical characterization of the plasma needle, New J. Phys. 6 (2004) 149.
[42] Suva, Grenzwerte am Arbeitsplatz, Bereich Arbeitsmedizin 2015.
[43] A.-Y. Moon, S. Noh, S.Y. Moon, S. You, Feasibility study of atmospheric-pressure plasma treated air gas package for grape's shelf-life improvement, Curr. Appl. Phys. 16 (2016) 440e445.
[44] F.D.L. Almeida, R.S. Cavalcante, P.J. Cullen, J.M. Frias, P. Bourke, F.A.N. Fernandes, S. Rodrigues, Effects of atmospheric cold plasma and ozone on prebiotic orange juice, Innov. Food Sci. Emerg. Technol. 32 (2015) 127–135.
[45] B.G. Dasan, I.H. Boyaci, M. Mutlu, Inactivation of aflatoxigenic fungi (Aspergillus spp.) on granular food 3 model, maize, in an atmospheric pressure fluidized bed plasma system, Food Control (2016), https://doi.org/10.1016/j.foodcont.2016.05.015.
[46] T. Kisch, A. Helmke, S. Schleusser, J. Song, E. Liodaki, F.H. Stang, P. Mailaender, R. Kraemer, Improvement of cutaneous microcirculation by cold atmospheric plasma (CAP): results of a controlled, prospective cohort study, Microvasc. Res. 104 (2016) 55–62.
[47] R. Brandenburg, H. Lange, T. von Woedtke, M. Stieber, E. Kindel, J. Ehlbeck, K.D. Weltmann, Antimicrobial effects of UV and VUV radiation of nonthermal plasma jets, IEEE Trans. Plasma Sci. 37 (6) (2009) 877–883.
[48] E. Stoffels, I.E. Kieft, R.E.J. Sladek, M.A.M.J. Van Zandvoort, D.W. Slaaf, Cold gas plasma in biology and medicine, in: R. d´Agostino, P. Favia, Y. Kawai, H. Ikegami, N. Sato, F. Arefi-Khonsari (Eds.), Advanced Plasma Technology, Wiley-VCH Verlag GmbH & Co., KGaA, Weinheim, 2008, pp. 301–318.
[49] Z. Fang, C. Ruan, T. Shao, C. Zhang, Two discharge modes in an atmospheric pressure plasma jet array in argon, Plasma Sources Sci. Technol. 25 (2016) 01LT01.
[50] 〈http://www.mhtl.uwaterloo.ca/old/onlinetools/airprop/airprop.html〉.
[51] G. Ben-Dov, J. Cohen, Critical reynolds number for a natural transition to turbulence in pipe flows, Phys. Res. Lab. 98 (2007) 064503.
[52] VDI-Wärmeatlas, Wärmeübertragung bei der Strömung durch Rohre, Ga1, 10. Auflage, Springer-Verlag, Berlin-Heidelberg, 2006.
[53] R.M. Fish, L.A. Geddes, Conduction of electrical current to and through the human body: a review, Open Access J. Plast. Surg. (2009).
[54] W.H. Olsen, Electrical safety, in: G. John (Ed.), Medical Instrumentation Application and Design, 4th ed., Webster, 2009, pp. 638–675 (ISBN-13 978-0-471-67600-3).
[55] G. Faure, S.M. Shkol'nik, Determination of rotational and vibrational temperatures in a discharge with liquid non-metallic electrodes in air at atmospheric pressure, J. Phys. D: Appl. Phys. 31 (1998) 1212–1218.
[56] X. Lu, G.V. Naidis, M. Laroussi, S. Reuter, D.B. Graves, K. Ostrikov, Reactive species in non-equilibrium atmospheric-pressure plasmas: generation, transport, and biological effects, Phys. Rep. 630 (2016) 1–84.
[57] J. Winter, R. Brandenburg, K.-D. Weltmann, Atmospheric pressure plasma jets: an overview of devices and new directions, Plasma Sources Sci. Technol. 24 (064001) (2015).
[58] S. Hübner, J. Santos Sousa, V. Puech, G.M.W. Kroesen, N. Sadeghi, Electron properties in an atmospheric helium plasma jet determined by Thomson scattering, J. Phys. D: Appl. Phys. 47 (432001) (2014).
[59] J.-P. Boeuf, L.L. Yang, L.C. Pitchford, Dynamics of a guided streamer ('plasma bullet') in a helium jet in air at atmospheric pressure, J. Phys. D: Appl. Phys. 46 (015201) (2013).
[60] D. Riès, G. Dilecce, E. Robert, P.F. Ambrico, S. Dozias, J.-M. Pouvesle, LIF and fast imaging plasma jet characterization relevant for NTP biomedical applications, J. Phys. D: Appl. Phys. 47 (275401) (2014).
[61] D. Li, A. Nikiforov, N. Britun, R. Snyders, M.G. Kong, C. Leys, OH radical production in an atmospheric pressure surface micro-discharge array, J. Phys. D: Appl. Phys. 49 (455202) (2016).
[62] N. Bibinov, P. Rajasekaran, P. Mertmann, D. Wandke, W. Viöl, P. Awakowicz, Basics and biomedical applications of Dielectric Barrier Discharge (DBD), in: A.N. Laskovski (Ed.), Biomedical Engineering, Trends in Materials Science, InTech, 2011, pp. 123–150, , https://doi.org/10.5772/13192.
[63] M.S. Mann, R. Tiede, K. Gavenis, G. Daeschlein, R. Bussiahn, K.-D. Weltmann, S. Emmert, Th von Woedtke, R. Ahmed, Introduction to DIN-specification 91315 based on the characterization of the plasma jet kINPen® MED, Clin. Plasma Med. 4 (2016) 35–45.
[64] S. Emmert, F. Brehmer, H. Hänßle, A. Helmke, N. Mertens, R. Ahmed, D. Simon, D. Wandke, W. Maus-Friedrichs, G. Däschlein, M.P. Schön, W. Viöl, Atmospheric pressure plasma in dermatology: ulcus treatment and much more, Clin. Plasma Med. 1 (2013) 24–29.
[65] G. Isbary, G. Morfill, J. Zimmermann, T. Shimizu, W. Stolz, Cold atmospheric plasma a successful treatment of lesions in hailey-hailey disease, Arch. Dermatol. 147 (4) (2011) 388–390.
[66] G. Isbary, J. Heinlin, T. Shimizu, J.L. Zimmermann, G. Morfill, H.-U. Schmidt, R. Monetti, B. Steffes, W. Bunk, Y. Li, T. Klaempfl, S. Karrer, M. Landthaler, W. Stolz, Successful and safe use of 2 min cold atmospheric argon plasma in chronic wounds: results of a randomized controlled trial, Br. Assoc. Dermatol. 167 (2012) 404–410.